# BIOLOGICAL EVALUATION AND *IN SILICO* STUDIES OF PYRIDYLPYRAZOLECARBOXYLIC ACID: SYNTHESIS AND CHARACTERIZATION

**P. Madhu[a*], S. Jeevitha[a], Rajendran Sribalan[b]**

**Abstract**

Pyridylpyrazolecarboxylic acid (**PPC**) was synthesized and the structure was confirmed by $^{1}H$ NMR, $^{13}C$ NMR, Mass and FT-IR spectroscopic techniques. The *in vitro* antioxidant and anti-inflammatory activities were screened for **PPC.** It showed nearer anti-inflammatory and antioxidant activities towards the standard drugs. Further, the **PPC** was performed for molecular docking and molecular modelling to compare the biological activities for additional support.

**Keywords:** Pyridylpyrazolecarboxylic acid, Antioxidant, Anti-inflammatory, Molecular electrostatic potential, Molecular docking study.

**Highlights**

- The biologically active **PPC** was synthesized and characterized by different spectroscopic techniques.
- **PPC** showed nearer anti-inflammatory and antioxidant activities towards the standard drugs.
- Molecular electrostatic study and Molecular docking study supports the biological activity of **PPC**.

**Graphical abstract**

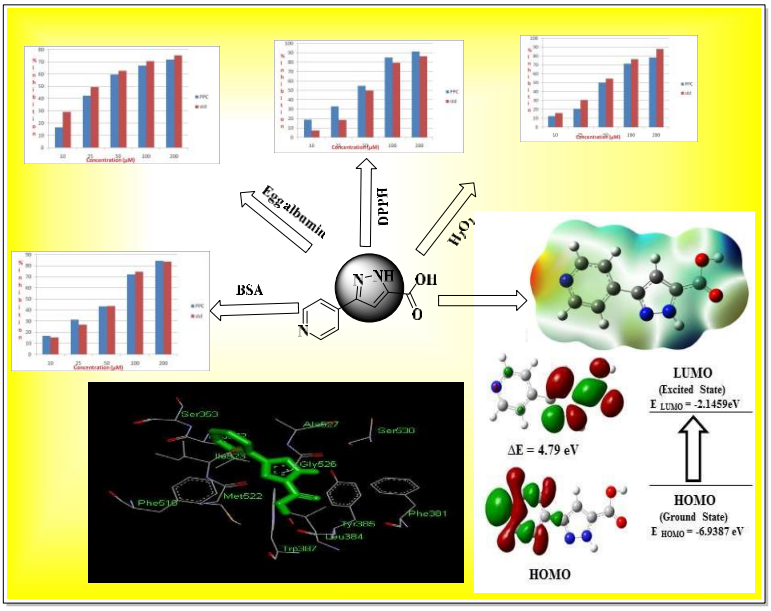


[a]Department of Chemistry, Thiruvalluvar Government Arts College, Rasipuram-637 401, Tamil Nadu, India
[b]Biochemie Innovations Laboratory, Tindivanam-604 001, Tamil Nadu, India

***Corresponding Author:** P. Madhu
[*]Department of Chemistry, Thiruvalluvar Government Arts College, Rasipuram-637 401, Tamil Nadu, India
Email: madhup.chem@gmail.com, Tel: +91 9944502310

**DOI:** 10.53555/ecb/2023.12.12.261

## 1. Introduction

Many heterocyclic compounds are found in natural products and biomolecules, which play a vital role in biochemical processes [1-2]. Heterocyclic compounds used in the medicines are as amino acids like histidine, proline and tryptophan. Vitamins and coenzymes precursors such as pyridoxine, folic acid, thiamine, riboflavin, biotin and B12 were also containing heterocyclic units. There is numeral pharmacologically active heterocyclic compounds that have been synthesized and many of them are in regular clinical use [3]. Literature survey shows that many of the heterocyclic moieties such as thiazolidinones, thiazoles, pyrazolines show very good biological activities [4].

Amid, nitrogen containing heterocyclic compounds like pyridine and pyrazole has been used in several fields [5-6]. Pyrazole and its derivatives have widespread potential pharmacological activities (Fig. 1) such as antitumor [7], anti-inflammatory [8], antiviral [9] and antimicrobial activity [10]. Pyrazole derivatives of celecoxib [11] and deracoxib [12] are used as selective COX-2 inhibitors. Recently, Kasımogulları et al. described that pyrazole-3-carboxylic acid derivative which is proven as anti-proliferative [13]. Chuang et al. reported the pyrazole incorporated pyridine and arene sulfonyl moiety exhibited anti-HBV agents in HepG2 cells [14]. Piyush N. Kalaria et al. synthesized biologically active fused heterocyclic compounds using pyrazole moiety [15]. Similar to pyrazole, pyridine nuclei have various pharmacological activities like anticancer [16], antibacterial [17], antifungal [18], anti-inflammatory [19], antidepressant [20] and antiviral activity [21].

Carboxylic acid plays a key role in living systems as well as in drug design. For instance, amino acids and prostanoids contain the carboxylic acid moiety. Several drugs containing carboxylic acid which have been marketed worldwide [22-23]. The strong electrostatic interactions and a hydrogen bonding interaction are the reason for the drug-target interactions of carboxylic acid.

Based on the importance of these active moieties, the research is focused to synthesize pyridylpyrazole carboxylic acid (**PPC**). This synthesized **PPC** was studied for their antiinflammatory and antioxidant activities. In silico studies such as molecular docking and quantum mechanical modelling were carried out for **PPC**. The experimental studies have been accompanied by computational studies, for understanding the behavior of the **PPC** and identification of the important information about the **PPC**.

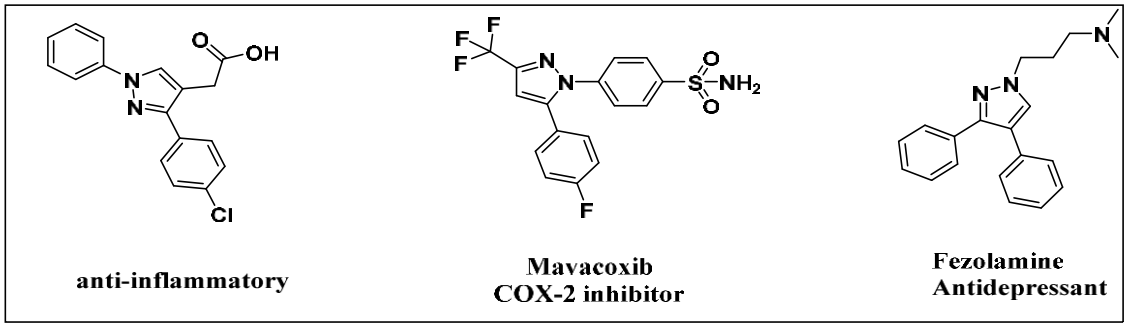


Fig. 1. Pyrazole containing drugs

## Experimental section

### Materials and Instrumentation

All chemicals were purchased from Sigma-Aldrich and Merck and used as received without further purification. The solvents used were analytical grade and double distilled water was used throughout the experiment. The progress of all the reactions was monitored by TLC using silica gel 60F254 and visualized under UV 254-366 nm and iodine. $^{1}$H NMR (300MHz) and $^{13}$C NMR (75MHz) were recorded on Bruker NMR instrument in $CDCl_3$ and DMSO-$d_6$ as solvents and TMS as an internal standard. Electron spray ionization mass spectra (ESI-MS) were recorded on LCQ Fleet mass spectrometer (Thermo Fisher Instruments Ltd., US). Shimadzu UV-1800 UV-Vis spectrometer was used to record UV absorption spectra for biological activities.

### Synthesis

The PPC was synthesized by following the reported method by Sribalan et al. [24]

Synthesis of ethyl 2,4-dioxo-4-(pyridin-4-yl)butanoate (2)

$^{1}$H NMR (300 MHz, $CDCl_3$) δ 8.78 (d, J = 5.5 Hz, 2H), 7.85 (d, J = 5.5 Hz, 2H), 4.42 (q, J = 14.0, 7.1 Hz, 2H), 1.42 (t, J = 7.0 Hz, 3H). $^{13}$C NMR

(75 MHz, $CDCl_3$) δ 192.89, 173.26, 165.10, 150.57, 137.70, 122.79, 61.75, 29.62, 14.15.
Synthesis of ethyl 3-(pyridin-4-yl)-1H-pyrazole-5-carboxylate (3)
$^1$H NMR (300 MHz, DMSO-$D_6$) δ 14.36 (s, 1H), 8.64 (d, J = 5.7 Hz, 2H), 7.85 (d, J = 5.7 Hz, 2H), 7.51 (s, 1H), 4.36 (q, J = 14.0, 7.0 Hz, 2H), 1.34 (t, J = 7.1 Hz, 3H). $^{13}$C NMR (75 MHz, DMSO-$D_6$) δ 163.78, 150.81, 135.88, 127.73, 120.08, 107.35, 61.33, 14.68.
Synthesis of 3-(pyridin-4-yl)-1H-pyrazole-5-carboxylic acid (**PPC**)
$^1$H NMR (300 MHz, DMSO-$D_6$) δ 8.93 (bs, 2H), 8.47 (d, J = 5.3 Hz, 2H), 7.80 (s, 1H).
$^{13}$C NMR (75 MHz, DMSO-$D_6$) δ 160.58, 148.04, 142.48, 122.51, 109.74. ESI-Mass: calculated m/z 189.05 found 190.11 $(M+1)^+$. IR$cm^{-1}$: 3190, 3120, 2960, 2860, 1700, 1630, 1430, 829, 746.

**Biological studies**
**Anti-inflammatory activity:**
The anti-inflammatory procedure was carried out by following the reported literature [25].
**Antioxidant activity:**
The antioxidant procedure was carried out by following the reported literature [25].

**Molecular docking study**
The molecular docking studies were performed by using Autodock software [30]. The three-dimensional structure of **PPC** was constructed using ChemBio 3D ultra 13.0 software, and then they were energetically minimized using MMFF94 with a maximum number of iterations of 5000 and a minimum RMS gradient of 0.10 [31]. The crystal structures of Protein (PDB ID: 1PGG and 4-COX) were taken from the Protein Data bank (www.rcsb.org). The docked complexes were visualized using the discovery studio 4.1 client.

**DFT Calculation and Molecular electrostatic map potential:**
The computational calculations of the Highest occupied molecular orbital (HOMO) and Lowest unoccupied molecular orbital (LUMO) in the checkpoint files were performed with Gaussian 09 W program using density functional theory [32]. The chemical structure of the compound was optimized with B3LYP/6.311 ++ G (d,p) basis set. To visualize the computed structures including HOMO, LUMO and Molecular electrostatic potential (MEP) representations the Gauss view software package was used.

**Results and discussions Chemistry**
The **PPC** was synthesized by following the reported method which is described in scheme 1 [24]. The precursor 4-acetylpyridine reacts with diethyloxalate in the presence of sodium hydride giving the intermediate 2. The reaction of intermediate 2 with hydrazine hydrate yielded pyridylpyrazole ester 3. The acid hydrolysis of ester 3 gave **PPC**. The **PPC** was characterized by different spectroscopic techniques. The $^1$H NMR clearly showed that the **PPC** contains 3 sets of protons (Pyrazole NH and Carboxylic acid may not appear). The peaks appeared at 8.93 and 8.46 ppm due to the presence of a pyridyl unit. The singlet at 7.80 ppm showed the presence of pyrazolyl CH unit. The $^{13}$C NMR showed 5 sets of carbon signals (2 quaternary carbon signals may not appear). The peak at 160.57 ppm showed the presence of carboxylic acid carbon. In the ESI-Mass spectrum, the parent ion peak appears at 190.11 in the positive mode. The IR spectrum also gave some additional evidence for the **PPC** formation. The stretching frequency at 3190 $cm^{-1}$ indicates the presence of pyrazolyl NH. The stretching frequency at 3120 $cm^{-1}$ appeared due to the OH stretching frequency of carboxylic acid. The absorption band from 2860 to 3040 $cm^{-1}$ indicates the presence of aromatic CH units. The sharp peak at 1700 $cm^{-1}$ indicates the presence of carbonyl unit of carboxylic acid. The IR spectrum was also calculated theoretically and compared with the observed spectrum. The calculated and observed spectrum of **PPC** is given in Fig. S1. Calculated and observed frequencies are given in Table S1.

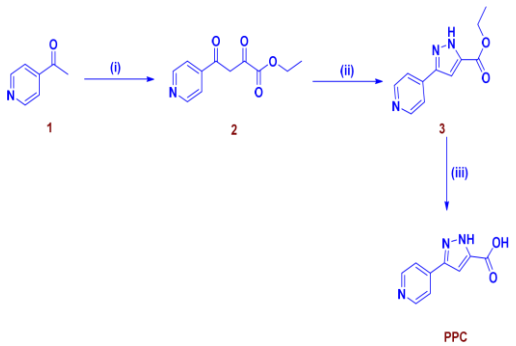


**Reagents and conditions:** (i) NaH, Diethyloxalate, DMF, 1h, RT; (ii) $NH_2NH_2.H_2O$, ethanol, 24h, RT; (iii) 6N HCl, 6h, reflux

**Scheme 1:** Synthetic route of the **PPC**

**Biological studies**
*In vitro* Anti-Inflammatory activity (BSA denaturation and egg albumin denaturation technique)

**BSA denaturation technique**

Protein denaturation is a loss of biological properties of protein molecules. Protein denaturation is responsible for the cause of inflammation like rheumatoid arthritis. The protein denaturation mechanism is involved in the alteration of electrostatic force, hydrogen bond, hydrophobic and disulfide bonds. Hence the prevention of protein denaturation may be used in preventing inflammation [25].

The present study showed that the BSA anti-denaturation activity of **PPC** on inhibiting the BSA denaturation is shown in Fig. 2. Their absorbance was measured at 660 nm by using a UV-visible spectrophotometer. The experimental results were compared with diclofenac sodium drug at different concentrations such as 10, 25, 50, 100 and 200 µM respectively. The maximum inhibition of 84.53 % was observed in **PPC** at the concentration of 200 µM which is equal to the standard drug diclofenac sodium. Moreover, various concentrations of the synthesized compound showed equal activity to the standard diclofenac sodium drug. From these observations, the **PPC** showed very good anti-denaturation activity.

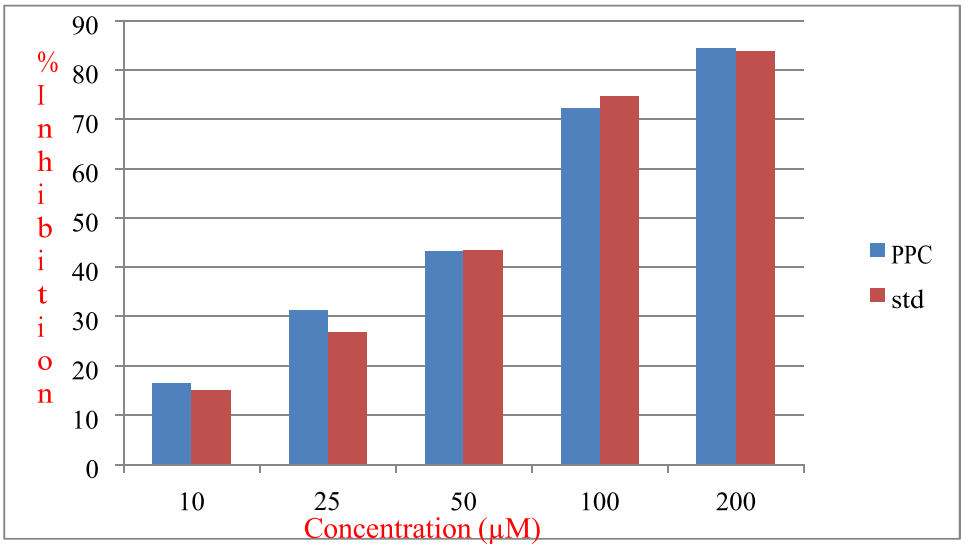


**Fig. 2.** Anti-inflammatory activity (BSA) of **PPC**.

**Egg albumin denaturation technique**

The **PPC** was also studied for *in vitro* anti-inflammatory activity using the egg albumin denaturation technique. Different concentrations of **PPC** were prepared for this study (10 to 200 µM). Diclofenac sodium drug is used as a standard to compare the activity of **PPC**. Similar to the bovine serum albumin assay, the **PPC** showed nearer activity to standard. The % inhibition was represented in Fig. 3. From these experiments, **PPC** has potent anti-inflammatory activity against bovine serum albumin and egg albumin.

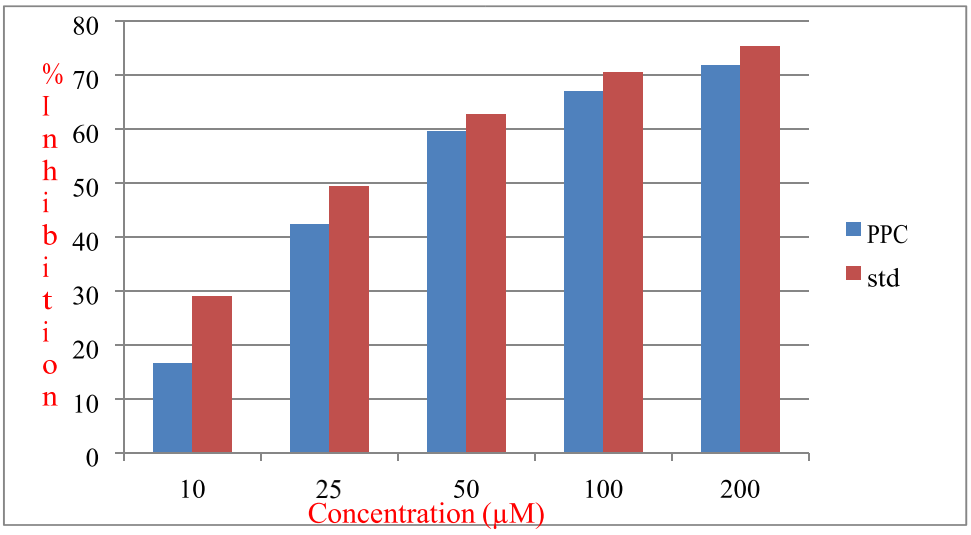


Fig. 3. Protein denaturation of **PPC** (egg albumin)

***In vitro* Antioxidant activity (DPPH radical scavenging and $H_2O_2$ scavenging study)**

**DPPH radical scavenging activity**

**PPC** was studied for antioxidant activity using DPPH radical scavenging assay. Generally, antioxidants react with DPPH which donates hydrogen and quench the DPPH radical. The color change was measured at 517 nm. The percentage of inhibition was tested for **PPC** along with standard ascorbic acid at different concentrations such as 10 µM, 25 µM, 50 µM, 100 µM and 200 µM respectively. Each test has been evaluated twice and the percentage of inhibition was represented in Fig. 4. In 10µM concentration, the **PPC** showed 18.6 % inhibition while the standard ascorbic acid showed low level percentage inhibition (7.18 %). Similarly, an increased concentration of PPC from 10 to 25 µM showed 32.87 % inhibition. But the standard ascorbic acid showed 18.37 %. Further increase in concentration enhanced the antioxidant activity than ascorbic acid. From the above results, it is clearly understood that the **PPC** has high DPPH free radical scavenging activity.

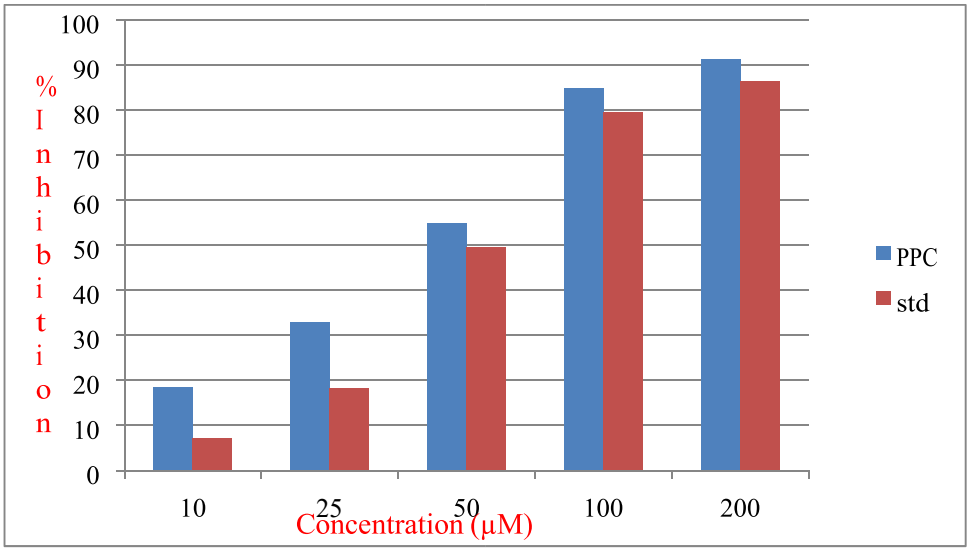


Fig. 4. Antioxidant activity (DPPH) of **PPC**.

**$H_2O_2$ scavenging activity**

Similarly, the **PPC** was tested against the $H_2O_2$ scavenging assay. The different concentrations of **PPC** and ascorbic acid were tested for this study (10, 25, 50,100, and 200 µM). The absorption of hydrogen peroxide is recorded at 230 nm. The % of inhibition of the **PPC** was represented in Fig. 5. From this experiment, the **PPC** showed nearer $H_2O_2$ scavenging activity to standard ascorbic acid at all concentrations.

The antioxidant activity results suggested that the **PPC** has very good DPPH radical scavenging activity and better $H_2O_2$ scavenging activity.

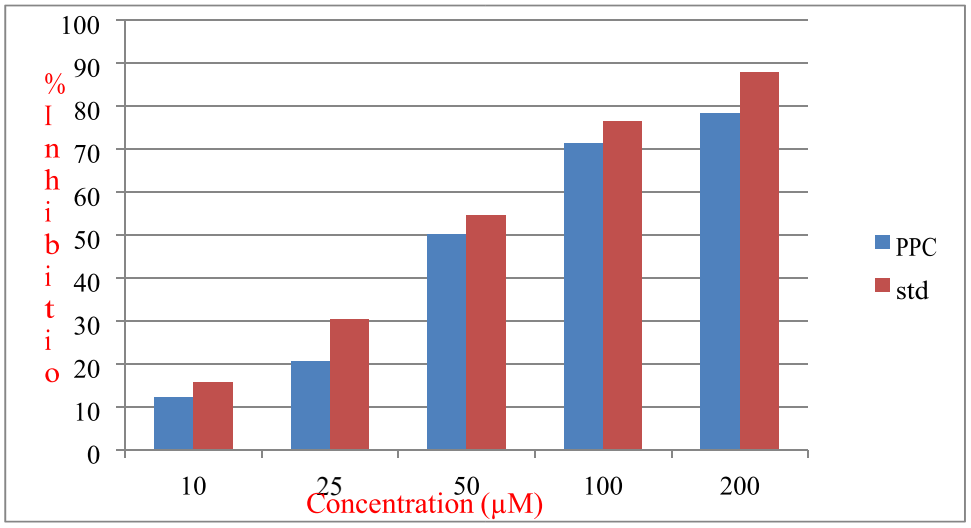


**Fig. 5.** Antioxidant activity ($H_2O_2$) of **PPC**.

**Frontier Molecular Orbital**

The highest occupied molecular orbital (HOMO) and lowest unoccupied molecular orbital (LUMO) are used to determine the way of interaction of the molecule. The highest occupied molecular orbital act as an electron donor and the lowest unoccupied molecular orbital acts as an electron acceptor [26]. The HOMO and LUMO energy is -6.9387 and -2.1459 eV. These negative energies indicate that the PPC is a stable molecule. Here, the HOMO has leading contributions from the pyridine ring whereas LUMO has major contributions in the pyrazole ring and carboxylic acid group. Hard and soft nucleophiles and electrophiles are closely related to the energies of HOMO and LUMO. Hard nucleophile has a low energy HOMO and soft nucleophile have a high energy HOMO, as well as hard electrophiles, have a high energy LUMO and soft electrophiles have a low energy LUMO [26]. **PPC** showed hard nucleophiles and electrophiles. Hardness and softness are used to measure the reactivity of the molecule and stability. **PPC** has a large HOMO-LUMO band gap (4.7928 ΔE). This band gap indicated that the molecule has good stability and large chemical hardness [27]. The electrophilicity index is useful to explain the binding capacity of the molecule. Here, **PPC** exhibits the highest electrophilicity index which confirms its highest capacity to accept electrons. The HOMO and LUMO of the **PPC** are represented in Fig. 6 and the frontier molecular orbital parameters were represented in Table 1.

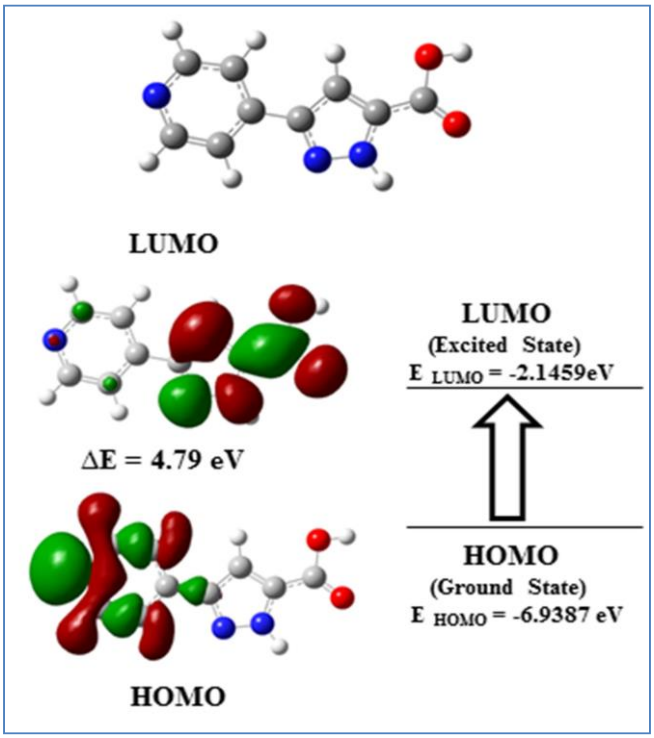


Fig. 6. Frontier molecular orbital of **PPC**

**Table 1 DFT calculation of PPC**

| S.No | Compound Name | HOMO | LUMO | Band gap | Chemical potential | Electro negativity | Global hardness | Global softness | Electro philicity index |
|---|---|---|---|---|---|---|---|---|---|
| 1 | PPC | -6.9387 | -2.1459 | 4.7928 | -4.5423 | 4.5423 | 2.3964 | 0.2086 | 4.3049 |

**Molecular Electrostatic potential**

The molecular electrostatic potential is used for predicting the region of electrophilic and nucleophilic sites and it was used to analyze the binding region of the molecule. In molecular electrostatic potential, the blue region represented the possible site for the electrophilic attack, while the red region implies the possible site for the nucleophilic attack [27]. Electrophilic and nucleophilic sites will be very useful for identifying the biological activity (enzyme binding) of the molecule. Particularly, the nucleophilic site (red color) of the molecule is more important because it is ready to make hydrogen bonding interaction with protein [28]. In PPC, the nucleophilic site is positioned on the

pyridyl ring. Similarly, in molecular docking studies, hydrogen bonding was observed in the pyridyl ring. So nitrogen can behave as an ideal hydrogen bonding donor group. Further, the pyrazole ring and carboxylic acid showed positive potential (electrophilic site). The molecular docking studies also revealed that the hydrogen bonding and pi-alkyl interaction occurs in the pyridine, pyrazole, and carboxylic acid group. Based on these results, we have concluded that these particular regions are responsible for biological activity. The Molecular electrostatic potential mappings were represented in Fig. 7.

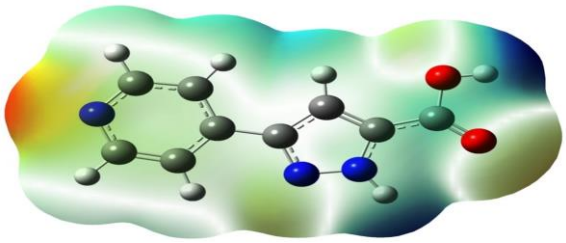

**Fig. 7.** Molecularelectrostatic potential of **PPC**.

**Molecular Docking Studies**

Docking studies were carried out by Auto-Dock Tool (1.5.6). Molecular docking of **PPC** was carried out with COX-1 and COX-2 [1PGG.pdb, 4COX.pdb] enzymes. The active site of 1PGG and 4COX is followed by the reported literature [29]. The crystal structure of COX-1 and COX-2 were taken from the protein data bank (www.rcsb.org). The **PPC** was found to have 5.98 kcal/mol binding energy and 41.66 µM inhibition constant. Albeit, the compound not shown any hydrogen bonding interaction with the active site of COX-1, it showed the least binding energy because it has other possible interactions such as pi-pi interaction, pi-alkyl interaction, and pi-sigma interaction. This docking pose analysis revealed that the pyridyl ring of **PPC** is oriented with pi-alkyl interactions surrounded by the side chains of Leu352, Ile523 and Ala527. Similarly, the carboxylic acid forms pi-alkyl interaction with Trp387, Leu384, Phe383, Tyr385, Trp387, Met522 and Leu384. Next, the pyrazole was found to have pi-pi T-shaped interaction with Tyr385 and Trp387 (Fig.8).

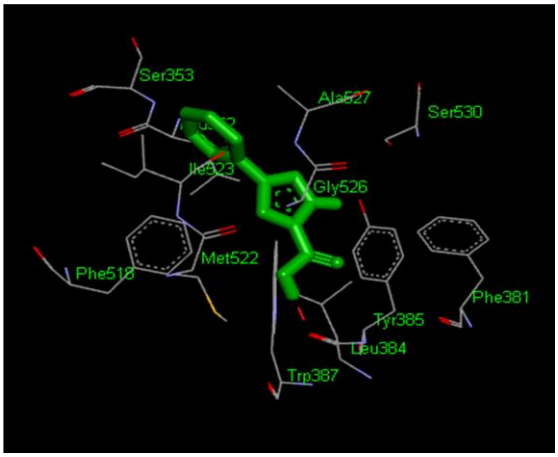


**Fig. 8.** Binding of **PPC** into the active site of COX-1.

**Table 2 Molecular docking interaction of synthesized compounds against 1PGG (COX-1)**

| S. No | Compound Name | | 1PGG (COX-1) | |
|---|---|---|---|---|
| | | Binding energy (kcal/mol) | Inhibition No. of constant H-bonding (µM) | H-bonded residue |
| 1 | **PPC** | -5.98 | 41.66 - | - |

Similarly, the **PPC** was docked with 4COX (COX-2). The PPC was found to have -5.94 kcal/mol binding energy and 44.24 µM inhibition constant along with two hydrogen bonding interactions. The Carbonyl group of carboxylic acid made hydrogen bonding interaction with Arg120 and the bonding distance was found to be 2.83Å. C2 carbon of pyridine forms a hydrogen bonding interaction with Met522 and the bonding distance was found to be 3.10Å.

Moreover, pyrazole ring forms pi-alkyl interaction and pi-sigma interaction with Ala527 and Val523. The pyridine ring showed the formation of pi-pi T-shaped interaction with Trp387 (Fig. 9).

From the docking studies, we have concluded that the hydrogen bond and Pi-pi alkyl interaction could be the sole reason for the biological activity of PPC. Binding energy, the number of hydrogen bonding, and the inhibition constant of 1PGG and 4COX were represented in Tables 2 and 3.

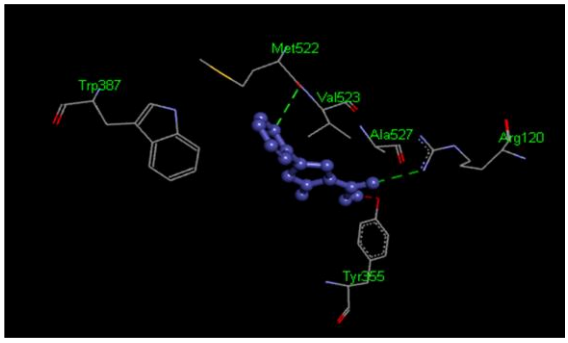


**Fig. 9.** Binding of **PPC** into the active site of COX-2.

**Table 3 Molecular docking interaction of synthesized compounds against 4COX (COX-2)**

| S. No | Compound Name | | 4COX (COX-2) | | |
|---|---|---|---|---|---|
| | | Binding energy (kcal/mol) | Inhibition constant (μM) | No. of H-bonding | H-bonded residue |
| 1 | PPC | -5.94 | 44.24 | 2 | Arg120, Met522 |

## Conclusion

The biologically active **PPC** was synthesized and well characterized by different spectroscopic techniques. The *in vitro* biological studies, as well as theoretical applications, proved that PPC may be used as a good bioactive molecule for anti-inflammatory and antioxidant activities. In vivo, studies also support its biological activity. The current research is focused to test the biological activity of **PPC** for other targets.

## Acknowledgement

We gratefully acknowledge the Tamil Nadu State Council for Higher Education (TANSCHE), India for financial support through Minor Research Project (1351/2019A).

## References:

1. S. Altürk, D. Avcı, O. Tamer and Y. Atalay, J. Mol. Struct., 1164, 28 (2018).
2. Y. Ju and R.S. Varma, J. Org. Chem., 71(2006) 135-141.
3. M.S. Saini, A. Kumar, J. Dwivedi and R. Singh, Int. J. Pharma Sci. Res., 4, 66 (2013).
4. A.A. Bekhit, A.M.M. Hassan, H.A.A. El-Razik, M.M.M. El-Miligy, E.J. El-Agroudy and A.E.-D.A. Bekhit, Eur. J. Med. Chem., 94, 30 (2015).
5. A. Ansari, A. Ali, M. Asif and Shamsuzzaman, New J. Chem., 41, 16 (2017).
6. S. Fustero, M. Sanchez-Rosello, P. Barrio and A. Simon-Fuentes, Chem. Rev., 111, 6984 (2011).
7. H.J. Park, K. Lee, S. Park, B. Ahn, J. C. Lee, H. Y. Cho and K. I. Lee, Bioorg. Med. Chem., Lett. 15, 3307 (2005).
8. A.K. Tewari and A. Mishra, Bioorg. Med. Chem., 9, 715 (2001).
9. S.L. Janus, M.A. Zahran, E.B. Pederson and C. Nielsen. Monatsh. Chem., 130, 1167 (1999).
10. P. Priyadarsini, B. Ujwala, C. Venkata Rao and V. Madhava Rao, Der Pharm. Lett., 4, 1123 (2012).
11. H. Cheng, K.M. Lundy DeMello, J. Li, S.M. Sakya, K. Ando, K. Kawamura, T. Kato, R.J. Rafka, B.H. Jaynes, C.B. Ziegler, R. Stevens, L.A. Lund, D.W. Mann, C. Kilroy, M.L. Haven, E.L. Nimz, J.K. Dutra, C. Li, M.L. Minich, N.L. Kolosko, C. Petras, A.M. Silivia and S.B. Seibel, Bioorg. Med. Chem. Lett., 16, 2076 (2006).
12. M.A. Chowdhury, K.R. A. Abdellatif, Y. Dong, D. Das, M.R. Suresh and E.E. Knaus, Bioorg. Med. Chem. Lett., 18, 6138 (2008).
13. R. Kasımogulları, H. Duran, A.S. Yaglioglu, S. Mert and I. Demirtas, Monatsh. Chem., 146, 1743 (2015).
14. H. Chuang, L.C. Sherlock Huang, M. Kapoor, Y-J. Liao, C. L. Yang, C.C. Chang, C.Y. Wu, J.R. Hwu, T.J. Huang and M.H. Hsu, Med.Chem. Comm., 7, 832 (2016).
15. P.N. Kalaria, S.C. Karad and D.K. Raval, Eur. J. Med. Chem., 158, 917 (2018).
16. A. Gangjee, Y. Zhu and S.F. Queener, J. Med. Chem., 41, 4533 (1998).
17. A.P. Krapcho, S.N. Haydar, S. T.-Chiott, M.P. Hacker, E. Menta and G. Beggiolin, Bioorg. Med. Chem. Lett., 10, 305 (2000).
18. M.J. Gil, M.A. Manu, C. Arteaga, M. Migliaccio, I. Encio, A. Gonzalez and V. Martinez- Merino, Bioorg. Med. Chem. Lett., 9, 2321 (1999).
19. P. Thirumurugan, S. Mahalaxmi and P.T. Perumal, J. Chem. Sci., 122, 819 (2010).
20. M.M. Naik, M.N. Deshpande, R. Borges, B.S Biradar and S.G Shingade, J. Drug Deliv. Ther., 7, 202 (2017).
21. F. Monna, F. Chimenti, A. Balasco, B. Bizzarri, W. Filippelli, A. Filippelli and L. Gagliardi, Eur. J. Med. Chem., 34, 245 (1999).
22. P. J. Hajduk, M. Bures, J. Praestgaard and S.W. Fesik, J. Med. Chem., 43, 3443 (2000).
23. C. Ballatore, D.M. Huryn and A.B. Smith, Chem. Med. Chem., 8, 385 (2013).
24. R. Sribalan, G. Banuppriya, M. Kirubavathi, A. Jayachitra and V. Padmini, Bioorg. Med. Chem. Lett., 26, 5624 (2016).
25. R. Sribalan, M. Kirubavathi, G. Banuppriya and V. Padmini, Bioorg. Med. Chem. Lett., 25, 4282 (2015).
26. M.H. Helal, S.A. El-Awdan, M.A. Salem, T.A. Abd-elaziz, Y.A. Moahamed , A.A.

ElSherif and G.A.M. Mohamed, Spectrochim. Acta, Part A., 135, 764 (2015).
27. Y.Tao, L. Han, X. Li, Y. Han and Z. Liu, J. Mol. Struct., 1108, 307 (2016).
28. A. Chidangil, M.K. Shukla and P.C. Mishra, Mol. Model.Ann., 4, 250 (1998).
29. N. Handler, W. Jaeger, H. Puschacher, K. Leisser and T. Erker, Chem. Pharm. Bull., 55, 64 (2007).
30. S.M.D. Rizvi, S. Shakil, and M. Haneef, Excli J., 12 (2013) 831–857.
31. Y.Y. Xu, Y. Cao, H. Ma, H.Q. Li and G.Z. Ao, Bioorg. Med. Chem., 21(2013) 388-394.
32. M.J. Frisch, G.W. Trucks, H.B. Schlegel, G.E. Scuseria, M.A. Robb, J.R. Cheeseman, J.A. Montgomery Jr., T. Vreven, K.N. Kudin, J.C. Burant, J.M. Millam, S.S. Iyengar, J. Tomasi, V. Barone, B. Mennucci, M. Cossi, G. Scalmani, N. Rega, G.A. Petersson, H. Nakatsuji, M. Hada, M. Ehara, K. Toyota, R. Fukuda, J. Hasegawa, M. Ishida, T. Nakajima, Y. Honda, O. Kitao, H. Nakai, M. Klene, X. Li, J.E. Knox, H.P. Hratchian, J.B. Cross, V. Bakken, C. Adamo, J. Jaramillo, R. Gomperts, R.E. Stratmann, O. Yazyev, A.J. Austin, R. Cammi, C. Pomelli, J.W. Ochterski, P.Y. Ayala, K. Morokuma, A. Voth, P. Salvador, J.J. Dannenberg, V.G. Zakrzewski, S. Dapprich, A.D. Daniels, M.C. Strain, O. Farkas, D.K. Malick, A.D. Rabuck, K. Raghavachari, J.B. Foresman, J.V. Ortiz, Q. Cui, A.G. Baboul, S. Clifford, J. Cioslowski, S.B.B. tefanov, G. Liu, A. Liashenko, P. Piskorz, I. Komaromi, R.L. Martin, D.J. Fox, T. Keith, M.A. AlLaham, C.Y. Peng, A. Nanayakkara, M. Challacombe, P.M.W. Gill, B. Johnson, W. Chen, M.W. Wong, C. Gonzalez, J.A. Pople, Gaussian 03, RevisionC.02, Gaussian, Inc., Wallingford, CT, (2004).

**Supplementary Information**

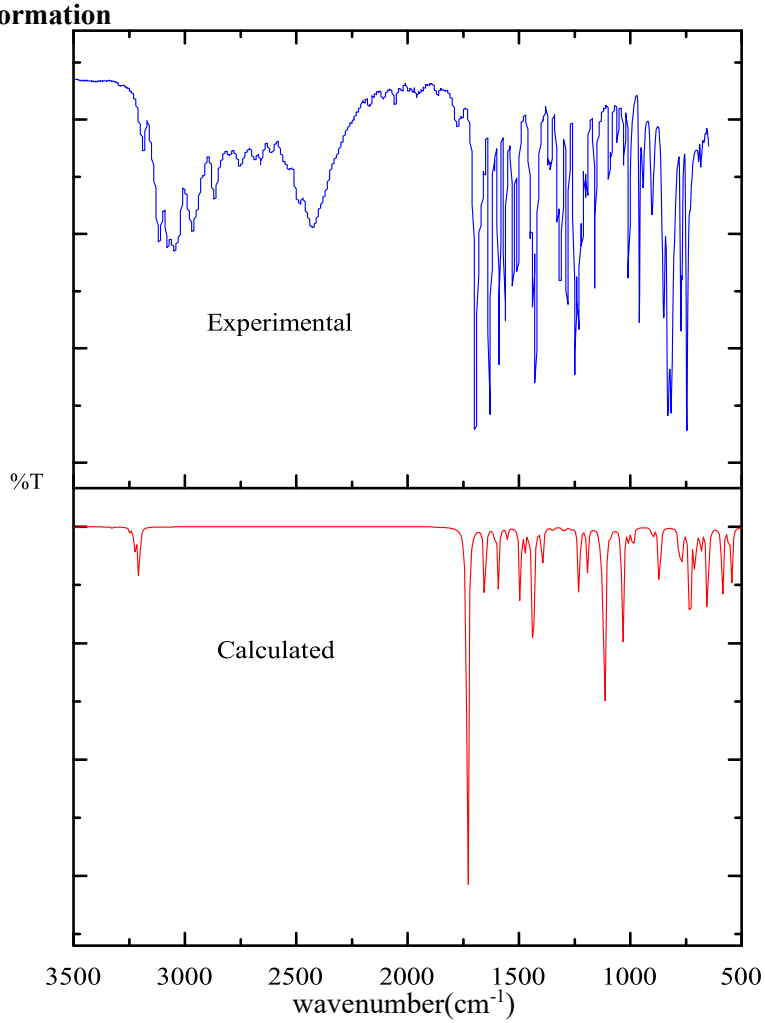


**Fig. S1.** Observed and calculated spectrum of PPC

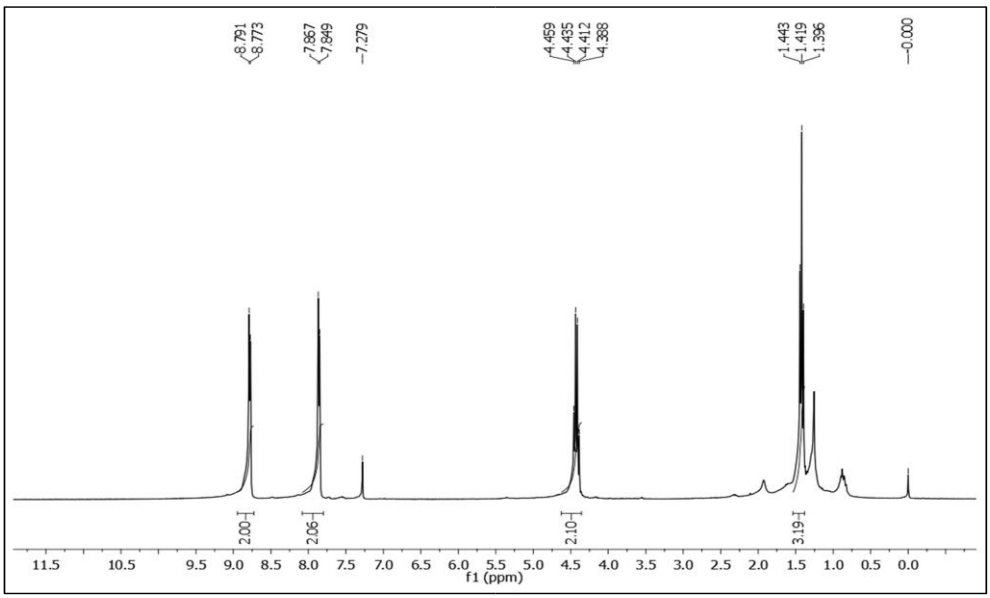


**Fig. S2.** $^{1}$H NMR (300MHz, $CDCl_3$) spectrum of compound 2

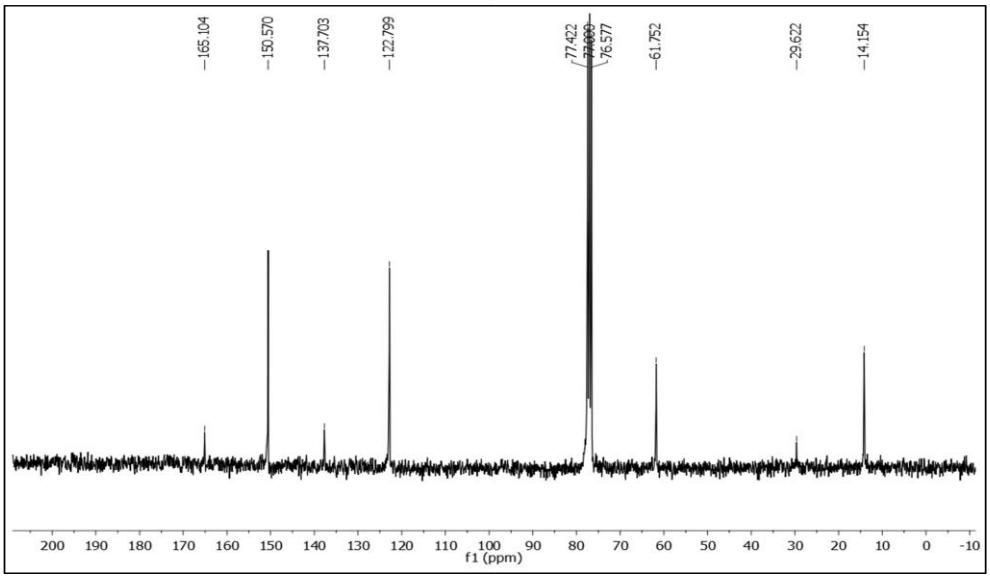


**Fig. S3.** $^{13}$C NMR (75MHz, $CDCl_3$) spectrum of compound 2

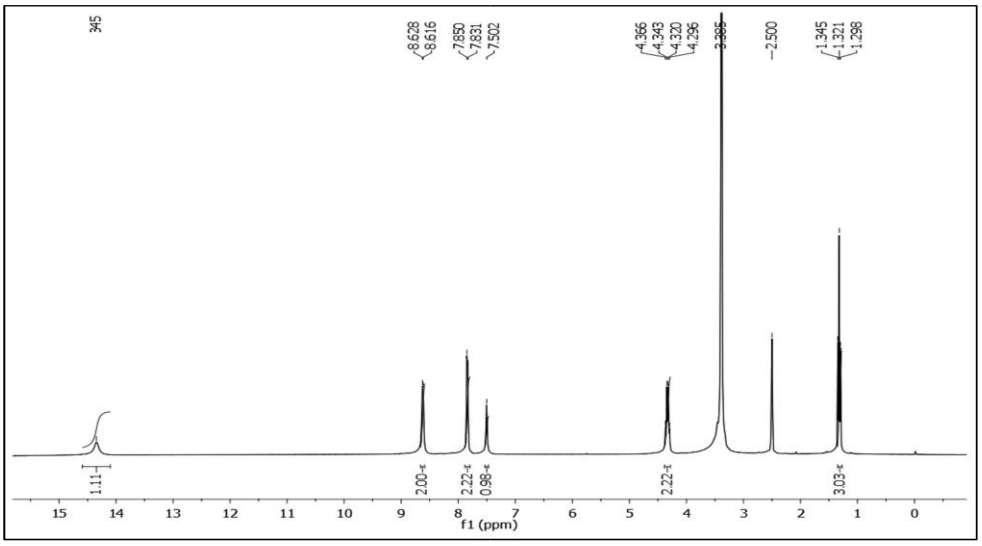


**Fig. S4.** $^{1}$H NMR (300MHz, DMSO-$D_6$) spectrum of compound 3

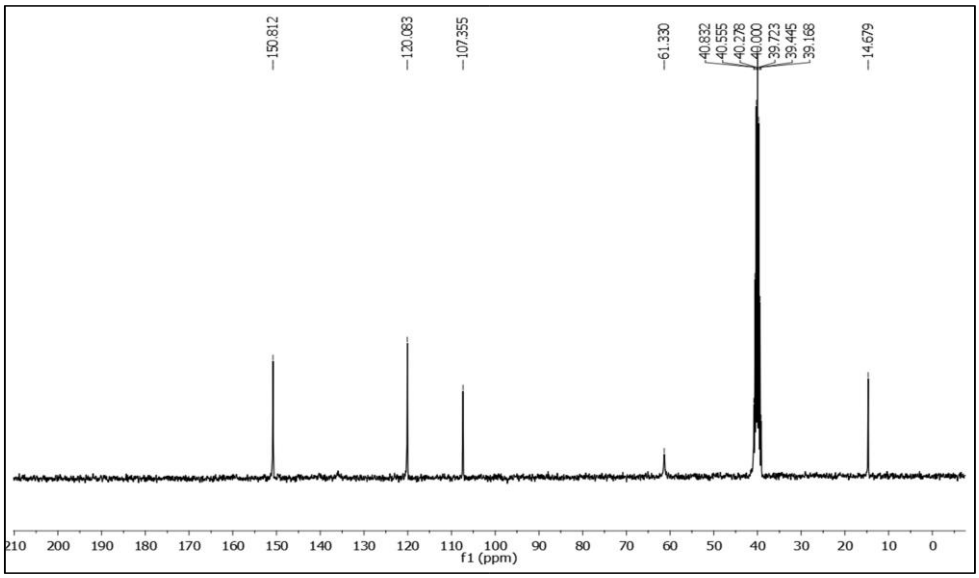


**Fig. S5.** $^{13}$C NMR (75MHz, DMSO-$D_6$) spectrum of compound 3

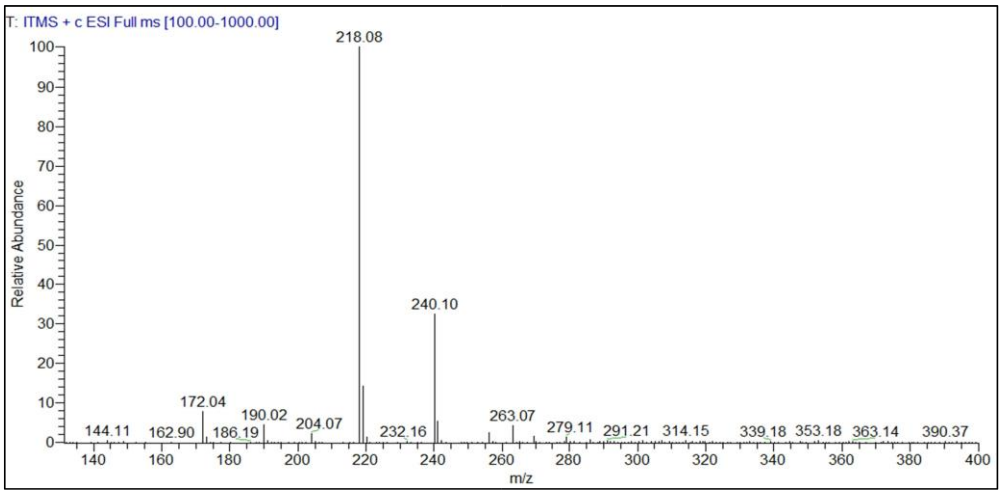


**Fig. S6**ESI-Mass spectrum of compound 3

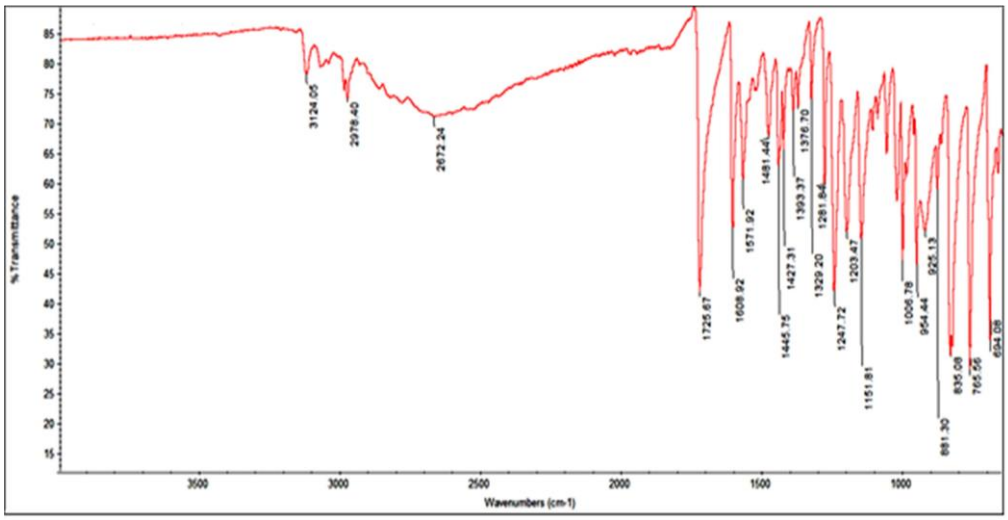


**Fig. S7.** FT-IR spectrum of compound 3

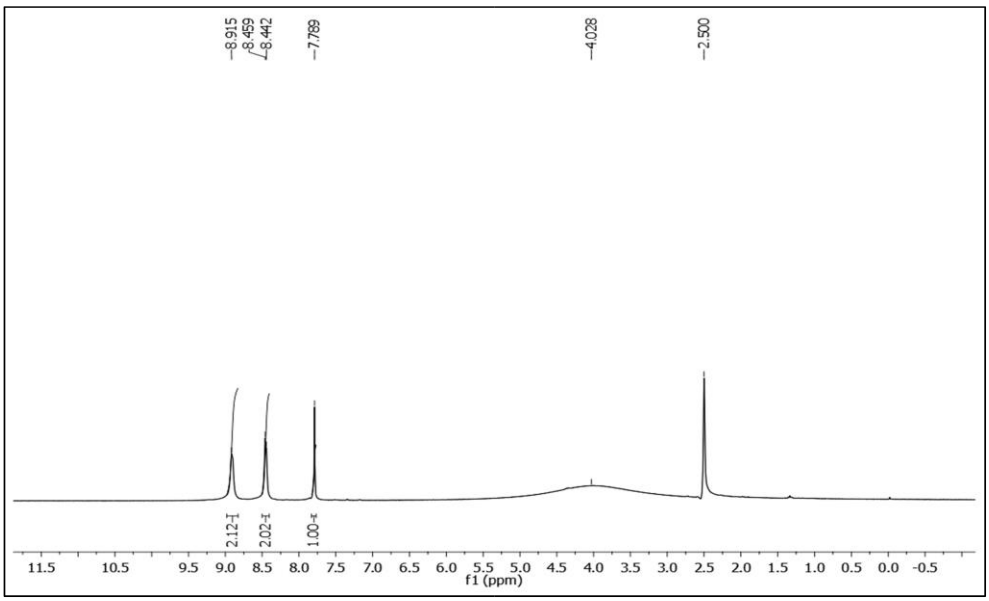


**Fig. S8.** $^{1}$H NMR (300MHz, DMSO-$D_6$) spectrum of compound PPC

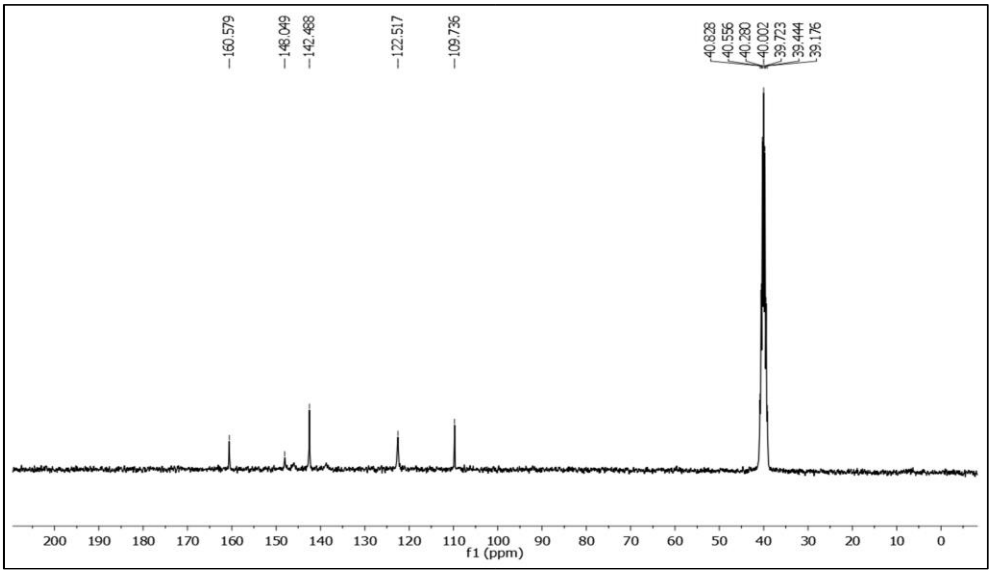


**Fig. S9.** $^{13}$C NMR (75MHz, DMSO-$D_6$) spectrum of compound PPC

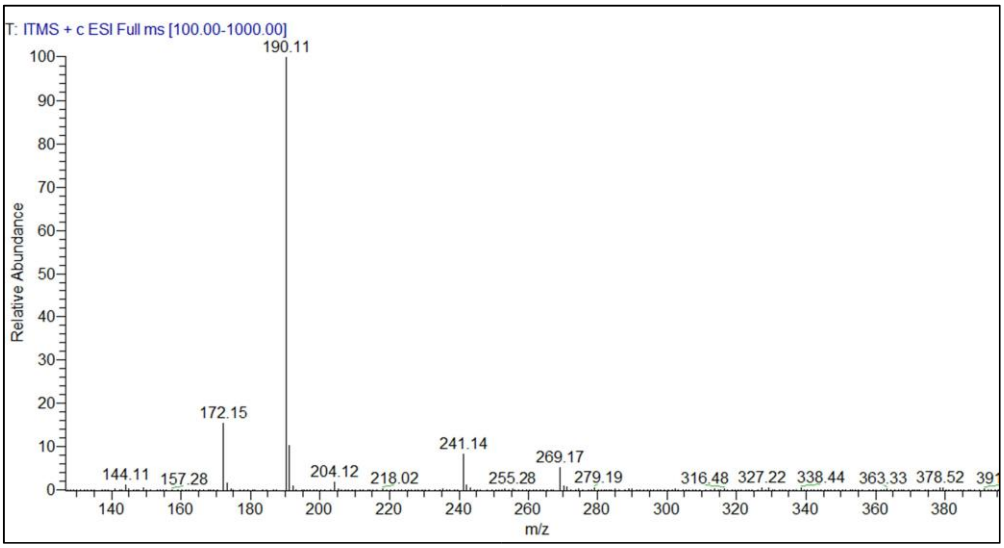


**Fig. S10**. ESI-Mass spectrum of compound PPC

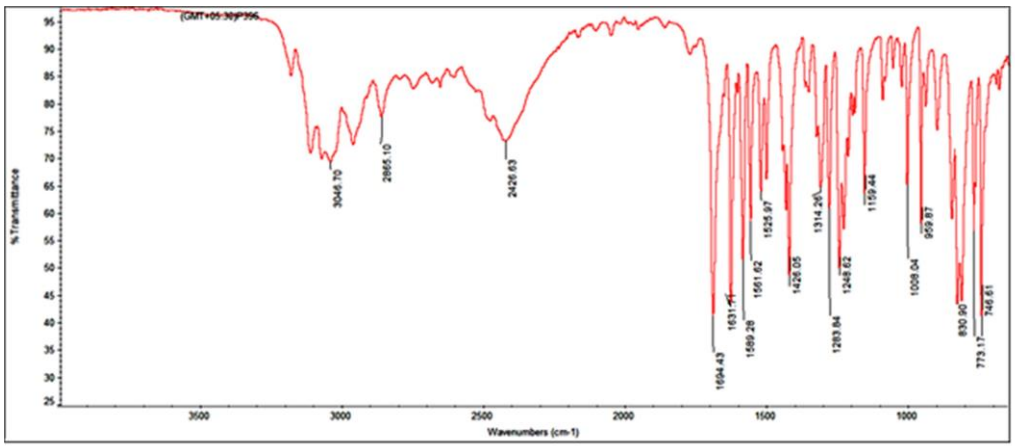


**Fig. S11 .**FT-IR spectrum of compound PPC

**Table S1.** Calculated and observed frequencies of PPC

| S.No. | observed | calculated | scaled | Vibrational assignment with PED (%) |
|---|---|---|---|---|
| 1 | | 3681 | 3538.542 | sOH(100%) |
| 2 | | 3628 | 3487.593 | sNH(100%) |
| 3 | 3190 | 3327 | 3198.242 | sCH(99%) |
| 4 | 3120 | 3247 | 3121.338 | sCH(93%) |
| 5 | | 3226 | 3101.151 | sCH(98%) |
| 6 | 3080 | 3210 | 3085.77 | sCH(87%),sNC(11%) |
| 7 | 3050 | 3203 | 3079.041 | sCH(94%) |
| 8 | 1700 | 1731 | 1664.009 | sOC(65%),sCC(15%) |
| 9 | 1630 | 1653 | 1589.027 | sCC(23%),bHCC(10%) |
| 10 | 1590 | 1610 | 1547.691 | sCC(33%) |
| 11 | 1560 | 1593 | 1531.349 | sNC(14%),sCC(21%) |
| 12 | 1530 | 1553 | 1492.897 | sCC(14%),bHCN(17%),bHCN(18%) |
| 13 | 1430 | 1494 | 1436.181 | sCC(13%),bNNC(19%) |
| 14 | | 1473 | 1415.993 | bHCC(10%) |
| 15 | | 1454 | 1397.729 | sCC(19%),sNC(12%),bHNN(18%),bHCN(11%) |
| 16 | 1360 | 1436 | 1380.425 | bHNN(27%),bHCN(12%) |
| 17 | 1320 | 1395 | 1341.012 | bHCN(16%),bHCN(15%),bHCC(14%),bHCC(18%) |
| 18 | 1280 | 1348 | 1295.831 | sNC(18%),bHOC(16%),bHCC(10%) |
| 19 | 1250 | 1300 | 1249.689 | sCC(13%),sNC(20%) |
| 20 | 1230 | 1288 | 1238.153 | sCC(13%),sNC(22%),sNN(10%) |
| 21 | | 1266 | 1217.005 | sNC(10%),bHCN(20%),bHCN(19%),bHCC(13%),b HCC(13%) |
| 22 | 1160 | 1230 | 1182.398 | sNC(18%),bHOC(12%),bHCC(13%) |
| 23 | 1100 | 1192 | 1145.868 | sNN(35%),bHOC(13%),bHCC(17%) |
| 24 | | 1131 | 1087.229 | sCC(17%),sCC(13%),bHCC(10%),bHCC(13%) |
| 25 | | 1115 | 1071.848 | sNN(13%),sOC(25%),bHOC(22%) |
| 26 | 1060 | 1107 | 1064.158 | bHCC(20%),bCCN(22%),bNCC(15%),bCNC(11%) |
| 27 | 1030 | 1087 | 1044.932 | sNN(10%),bCCN(13%).bHCC(25%) |
| 28 | | 1034 | 993.9832 | sCC(17%),sOC(19%)bCNN(25%) |
| 29 | | 1027 | 987.2541 | tHCNC(45%),tHCCC(35%),tCCNC(10%) |
| 30 | 960 | 1008 | 968.9894 | tHCNC(52%),tHCCN(23%),tCCCN(11%) |
| 31 | | 1007 | 968.0281 | sNC(23%),sNC(28%),bCCN(14%) |
| 32 | 943 | 988 | 949.7634 | bCCN(27%),bCNN(17%),bNNC(13%) |
| 33 | | 915 | 879.5886 | tHCNC(25%),tHCCC(31%),tHCCN(18%) |
| 34 | | 899 | 864.2078 | tHCCN(11%),tHCCN(43%) |
| 35 | 831 | 869 | 835.3688 | tHCNC(17%),tHCNC(12%),tHCCN(17%),tCCNN( 12%),oCCCC(15%) |
| 36 | 773 | 779 | 748.8519 | tHCCN(10%),tCCNC(10%),tCCCN(12%),tCNNC( |

| | | | | |
|---|---|---|---|---|
| | | | | 12%),oOCOC(27%) |
| 37 | 746 | 766 | 736.355 | tCCNC(12%),tCCCN(18%),oOCOC(29%) |
| 38 | | 734 | 705.5935 | tHNNC(49%),tHCCN(10%),tCNNC(17%) |
| 39 | | 730 | 701.7483 | sCC(11%),bCNC(29%) |
| 40 | 683 | 709 | 681.561 | tHNNC(43%),CNNC(35%) |
| 41 | | 696 | 669.0641 | bCCC(18%),bCCN(25%),bNCC(36%) |
| 42 | 648 | 683 | 656.5672 | sOC(14%),bOCO(33%),bCNC(11%) |
| 43 | | 653 | 627.7282 | tHOCC(32%),tCCNN(38%),oOCOC(22%) |
| 44 | | 586 | 563.3212 | tHOCC(57%),tCCNN(18%) |
| 45 | | 558 | 536.4048 | bNCC(13%),bCCC(19%),bOCC(24%) |
| 46 | | 545 | 523.908 | tCNNC(12%),oCCCC(29%) |
| 47 | | 448 | 430.662 | sCC(15%),bOCO(26%),bOCC(16%) |
| 48 | | 437 | 420.0877 | bNCC(24%),bCCC(31%),bOCC(19%) |
| 49 | | 394 | 378.7518 | tHCCN(12%),tCCNC(36%),tCNCC(26%),tCCCN(13%) |
| 50 | | 322 | 309.5383 | tCNCC(18%),tNNCC(36%),oCNCC(14%) |
| 51 | | 285 | 273.9702 | sCC(12%),sCC(25%),bCCC(14%),bOCO(10%),bNNC(11%) |
| 52 | | 200 | 192.2598 | bNCC(11%),bCCC(30%),bCCC(27%),bOCC(22%) |
| 53 | | 181 | 173.9951 | tCNCC(11%),oCNCC(38%),oCCCC(11%) |
| 54 | | 115 | 110.5494 | tOCCN(68%),oCCCC(10%) |
| 55 | | 93 | 89.40081 | bNCC(32%),bCCC(32%),bCCC(20%) |
| 56 | | 68 | 65.36833 | tNNCC(32%),tOCCN(19%),oCNCC(22%),oCCCC(15%) |
| 57 | | 32 | 30.76157 | tNCCC(88%) |

s: stretching, b: bending, t: torsional, o: out of plane bending.